LIQUID CRYSTAL ENGINEERING OF CARBON NANOFIBERS AND NANOTUBES

Christopher Chan, Kengqing Jian, Matt Sousa, Nancy Yang*, Yuming Gao, Hao Li, Brian Sheldon, Gregory Crawford, Robert Hurt

Brown University, Providence, RI
**Sandia National Laboratories, Livermore CA*

Much of the excitement surrounding new carbon nanomaterials can be traced to their *directional* properties, which arise through precise orientation of graphene layers[1,2] that are the anisotropic building blocks of all sp^2-hybridized carbon forms[3]. The high conductivity, strength, and stiffness of carbon nanotubes are directly related to the parallel orientation of graphene layers relative to the tube axis. Alternative crystal structures are seen in some cylindrical carbon nanoforms, including "platelet" nanofibers, whose graphene layers lie perpendicular to the fiber axis; and herringbone and cup-shaped nanofibers with tilted layer arrangements[1,4,5]. These platelet, herringbone, and cup-shaped nanofibers are inferior to "conventional" nanotubes/fibers in mechanical strength and conductivity, but contain exposed graphene edge sites that make them attractive for complementary applications such as catalysis[6,7] and Li intercalation electrochemistry[8]. A long term goal in carbon synthesis is to develop techniques for systematic control of graphene layer arrangement in order to fabricate "designer" materials and nanomaterials with crystal structures preprogrammed for specific applications[3].

Here we demonstrate a new approach for fabricating hollow carbon nanocylinders that are crystallographically inverted forms of "conventional" carbon nanotubes. Infiltration of polyaromatic solutions into nanochannel alumina followed by solvent evaporation deposits thin organic films on inner wall surfaces that can be covalently captured as sp^2-hybridized carbon structures. Nanochannel alumina has been used extensively in the past as a template for fabrication of nanofibers/tubes from polymers[9,10], metals[9], organic molecules[11] and carbons[12,13]. Here our goal is to use nanochannels not only for shape control, but also to direct the molecular structure of the material through polyaromatic/alumina surface interactions. We have previously used the discotic naphthalene polymer, AR mesophase, in combination with nanochannel alumina templates to produce unique carbon nanofibers, whose graphene layers lie perpendicular to the fiber axis[14]. This structure reflects the original (uncarbonized) discotic assembly[14], which is the only one that achieves the desired edge-on molecular anchoring on the inner alumina surfaces while also avoiding elastic director strain[14].

Here we strive to produce the first hollow nanoforms by this principle through the addition of solvents that create void volume upon evaporation. Solvent processing of high-MW polyaromatics is limited, however, by the strong intermolecular forces and low solubility. We therefore evaluated two competing approaches: (a) the *partial* dissolution of naphthalene polymer in strong aromatic solvents, pyridine and quinoline. The resulting solutions are rich in polyaromatic material but no longer exhibit liquid crystallinity due both to dilution and to the lower mean molecular weight of the soluble fraction, and (b) the use of indanthrone disulfonate aqueous solutions.

The latter polyaromatic precursor is synthesized by introducing sulfonic acid groups on the periphery of indanthrone (also "indanthrene"), a polyaromatic dye of planar discoid shape (see Fig. 1). In such amphiphilic discotic molecules the disk peripheries are hydrophilic, but the polyaromatic faces remain hydrophobic, and in aqueous solution the planar molecules stack face-to-face to provide favorable local environments for both faces and edge groups[15,16] (see Fig. 1). In indanthrone disulfonate solutions, this face-to-face stacking is extensive, leading to rod-like aggregates with aspect ratio near 200 having approximate diameters of 1.5 nm and mean lengths of 300 nm[16]. Proton dissociation imparts negative charge to the aggregates, which aids in their dispersion[16], and above 4-5% these solutions form lyotropic liquid crystalline phases in which the rod-like aggregates align by self-exclusion and electrostatic repulsion[16]. Coating optical substrates with concentrated lyotropic solutions in a manner that flow-aligns the rods is known to produce, upon drying, dichroic organic layers upon drying[17]. Dried films of indanthrone disulfonate have a density of 1.69 g/cm^3 by picnometry[17] and XRD analysis reveals crystallinity with a d-spacing of 0.336 nm in the _-stacks and molecular order parameters from 0.86-0.91[17]. For the present work indanthrone disulfonate was acquired as an ammonium salt solution from the firm Optiva (South San Francisco), which uses the solutions for fabrication of thin film organic polarizers[17].

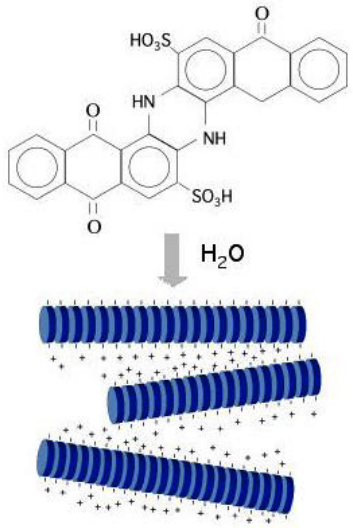

Fig. 1: Indanthrone disulfonate and its rod-like aggregates in aqueous solution.

Figures 2 and 3 show carbon nanotubes produced by capillary infiltration of ammonium indanthrone disulfonate solutions into nanochannel alumina followed by overnight drying and slow heating (4 C/min) to 700 C. The starting solutions of 2-12 wt-% lose most of their mass upon drying, leading to the formation of a thin film (2-12 molecular layers) on the inner surfaces of the 100 nm radius cylindrical template channels. The 700 C treatment converts the organic nanotubes into monodisperse carbon tubes of 100 nm radius and 60 _m length, which form free standing ordered arrays upon removal of the alumina template by 0.4 M NaOH etching (see Fig. 2A). Using 12 wt-% indanthrone disulfonate, the tubes show a cellular structure with hollow cavities separated by internal membranes. This bamboo-like cellular structure can be suppressed almost entirely by reducing solvent concentration from 12% to 2%. The lower concentration produces tubes with thinner walls and almost no internal structure.

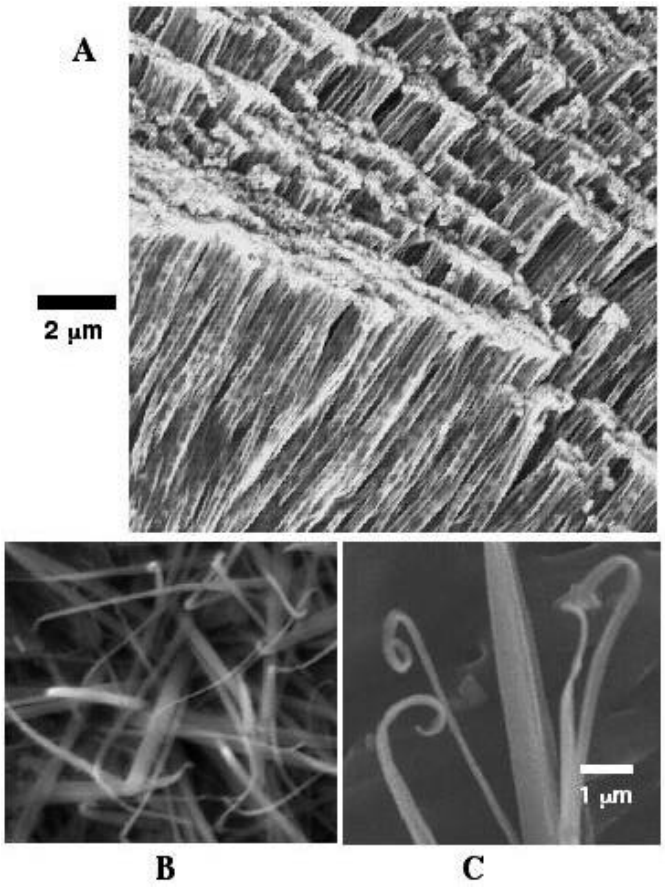

Fig. 2. Carbon nanotube array (A) and dispersed nanoribbons (B,C) formed by capillary infiltration of indanthrone disulfonate solutions into nanochannel alumina followed by thermal covalent capture at 700 C and template removal. The cellular nature of the tubes made at high solution concentration (12 wt-%) can be seen on the extended tube lengths at the bottom of panel A. The ribbons form in the presence of barium ions which reduce indanthrone disulfonate solubility.

High resolution fringe images reveal a unique crystallography in these thin-walled carbon nanotubes, in which the graphene layers orient *perpendicular* to the tube axis (Figure 3). The tube wall structure consists of short (2-3 nm) graphene layers with a statistical meandering about mean perpendicular orientation. These short meandering layers are typical for a low-temperature carbon derived from a liquid crystal precursor[3,14], and reflect the structure of the liquid crystalline phase at the point of solidification. The key feature in Fig. 3 is the uniform perpendicular alignment, which establishes the unique crystal orientation that characterizes this nanomaterial. Heat treatment of these phases can coalesce the layers and produce longer and straighter fringes, but does not alter the basic crystal symmetry established in the young, low-temperature carbon material[3].

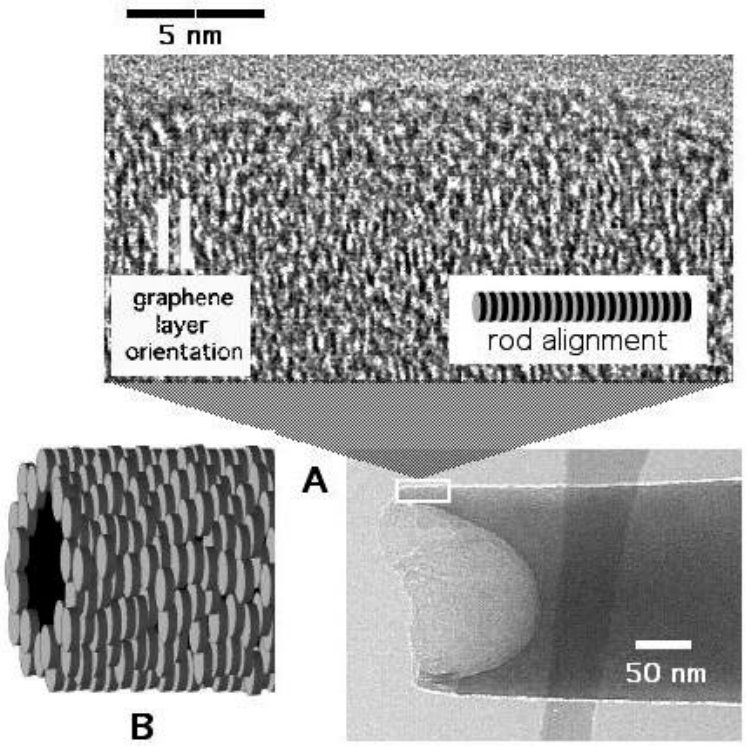

Figure 3. High-resolution TEM image shown the perpendicular graphene layer orientation in the walls of carbon nanotubes made from indanthrone-disulfonate solutions. The small and incompletely coalesced graphene layer segments observed here are typical for liquid-crystal derived carbons prepared at low temperatures (here: 700 C). The key feature is the uniform perpendicular alignment, which establishes the crystal orientation in this nanocarbon form. Panel B shows the inverted tube structure, where the molecular disk size is exaggerated for visibility.

We believe this unusual crystal structure is formed by orientational ordering of the rod-like supramolecules driven by configurational entropy as the rods become concentrated in the curved thin liquid films that coat the inner nanochannel walls during drying. The dried solid film of rod-like supramolecules is then covalently captured by thermal polymerization with accurate translation of the molecular order into an arrangement of linked graphene layers. The success of this covalent capture scheme could not be predicted *a priori*, as many thermal carbonization processes destroy supramolecular order in the organic precursor and/or alter the overall form of the carbon body though re-softening and volatile product release[3]. In separate thermogravimetric experiments we found that bulk samples of indanthrone disulfonate begin to decompose at around 300 C, at a point where the material retains most of its optical anisotropy. As heating continues sharp edges remain intact through 700 C indicating an all-solid-state carbonization path, and the final bulk carbons show multi-domain anisotropy. The absence of a liquid phase intermediate is also observed during the carbonization of

some other very-high-MW polyaromatics[18], and this property is likely key to the success of thermal covalent capture.

Two facts suggest that the original rod alignment occurs in the drying stage. First, the low precursor concentration at 2.25 wt-% is well below the concentration threshold (4-5 wt-%) needed for spontaneous orientation in the bulk[16], so under these conditions the rod-like aggregates are expected to be disordered in the original filled 100 nm radius capillaries. (Confinement effects will reduce the order/disorder threshold below 4-5 wt-%, but theoretical treatments of confined phase behavior show that shifts of these transition points are far too small to allow order at only one-half the threshold concentration in bulk.)

Secondly, we find by dipping the filled nanochannel membrane in 10 wt-% $BaCl_2$ solutions prior to drying and carbonization leads not to tubes but to nano-*ribbons* — continuous carbon strips of 60 _m in length, 200 nm in width with rectangular cross section (Fig. 2B,C). The divalent barium ion cross-links the negatively charged aggregates and reduces the solubility of the rod-like aggregates leading to early precipitation within the nanochannels rather than deposition on wall surfaces. HRTEM shows these ribbons to have a more random crystal structure suggesting that the rod-like molecular aggregates were not highly oriented in the solution at the point of precipitation prior to drying.

Figures 4 and 5 show the results for the other polyaromatic precursor, naphthalene polymer (AR mesophase, HP grade from Mitsubishi Gas Chemical). AR mesophase is an naphthalene oligomer with a distribution of molecular weights spanning 400 to 2000 Daltons with a mean of approximately 700 Daltons. Evaporation of the solvent (pyridine or quinoline) produces open-ended tubes (Fig. 4C). When saturated high-concentration (7.5 wt% in quinoline) solutions are employed (Fig. 4A), the cellular structure is especially pronounced. The hollow regions clearly appear to be vesicles, some of which show nearly regular spacing, and the overall structure can be described as a one-dimensional solid cellular foam. Increasing the drying time and maintaining temperature at 80 C (below the 113 C boiling point of quinoline) had little effect on the foam structure (Fig. 4B). Reducing the naphthalene polymer concentration to 1 wt-%, however, greatly suppresses this foam structure and produces instead hollow nanotubes (Fig. 4D). The 1D cellular foam thus appears to arise at high concentration where saturated conditions readily occur during drying leading to precipitation within and across the bulk channel rather than at a later stage in the thin drying film on inner wall surfaces.

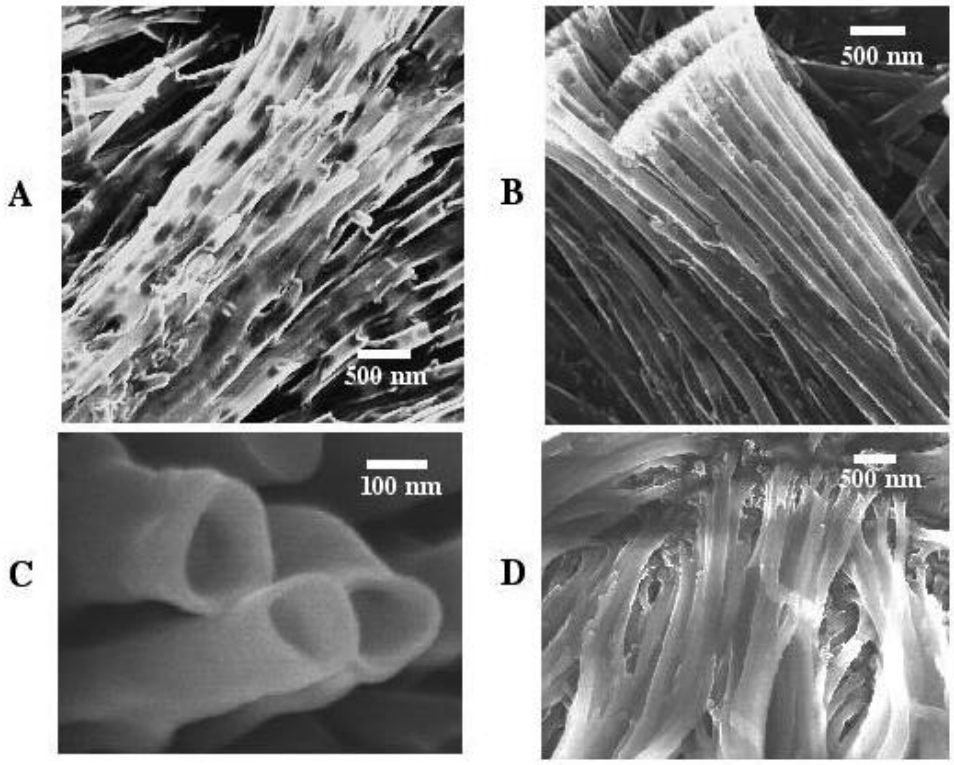

Figure 4. Cellulcar carbon nanotubes (A,B,C) and hollow carbon nanotubes (D) produced by solution processing of naphthalene polymer (AR mesophase). The hollow structure in (D) is the result of lower polyaromatic concentration (1 wt%) in quinoline solution compared to 7.5 wt-% for (A).

Figure 5 shows that the thin wall regions of the cellular tubes or foams have a similar graphene layer arrangement to the indanthrone-derived tubes — there is a strong preferential alignment *perpendicular* to the tube axis. It is remarkable that both precursors give this unusual structure, which suggests a general principle in polyaromatic assembly. In fact the same basic perpendicular symmetry is observed when AR naphthalene polymer is melt processed in nanochannel alumina into fully dense fibers[14]. Further, separate experiments show that the preferred surface anchoring state for AR mesophase is edge-on on flat substrates of alumina[19], as well as most other oxides, glasses, and metals[19]. We believe that the driving force for assembly of *each* of these structures is the preservation of internal ___ bonds, which are the strongest non-covalent interactions among large polyaromatics, and are stronger than _-surface interactions for most substrates[20]. The molecular structure shown in Figs. 3 and 5 (massive axial _-stacked columns) achieves the maximum extent of internal ___ bonding by exposing onlygraphene edges at the outer and inner wall surfaces. (Outward facing layers would force the loss of one set of internal ___ bonds). Further, the axial orientation of the columns avoids nanoscale curvature in the tangential direction.

By this mechanism, large planar polyaromatic precursors provide a natural route to new carbon forms with edge-rich surfaces, provided that the supramolecular order can be captured upon heating. The success of thermal capture hinges on the competition between melting and rotational diffusion on one hand, and thermal decomposition reactions that lead to covalent cross-linking and capture on the other. Many molecular assemblies undergo an order-disorder transition *first* and thus lose structure upon heating. In contrast, some polyaromatics larger than coronene (MW 300, m.p. 440 C) show sufficiently strong intermolecular forces to suppress melting through and past the thermal decomposition point[18]. The low molecular mobilities associated with this solid state carbonization can lead to retention of supramolecular order during carbonization. We cannot now predict which precursors will show this useful behavior, but it has been demonstrated for both AR naphthalene polymer (mean MW 700) and indanthrone disulfonate (MW 442) in confinement, making both systems attractive for covalent capture schemes.

Overall, polyaromatic solution processing can produce a unique set of high-aspect-ratio carbon nanoforms (tubes, ribbons, and 1D cellular foams) depending on synthesis conditions. The tubes and foams are crystallographically inverted and thus quite distinct from "conventional" carbon nanotube structures[1,2]. They possess the same basic crystal symmetry as "platelet" nanofibers[4,7], but are hollow, have tunable wall thickness, and show the meandering graphene layer structure that is unique to liquid-crystal-derived carbon. They exhibit graphene edge planes at both inner and outer surfaces and are interesting for a variety of applications where high-activity surfaces or access to interlayer spaces are advantageous. Promising application fields include catalysis[6,7], high discharge rate Li battery electrodes, and high-surface-density functionalization for selective adsorption or chemical sensing[21] using well-established graphene edge-site chemistry, which is often severely limited by edge-site availability.

Finally, indanthrone disulfonate is a promising new carbon precursor that offers a number of advantages for nanocarbon synthesis. As a polyaromatic liquid crystal it already possesses the basic graphite "kernel" in a mobile form that can be manipulated to achieve a high degree of molecular control over graphene layer arrangements. The use of the sulfonated aqueous form avoids the high melting and/or viscous phases typically associated with large polyaromatics by manipulating the secondary rod-like aggregates in solution, where mobility is achieved without the need to overcome ___ forces. The use of solvent rather than melt processing allows hollow forms to be assembled and the wall thickness to be tailored through selection of initial concentration. Finally the subsequent carbonization process for these confined phases preserves the supramolecular assembly without pressure or oxidative stabilization commonly used with other carbon precursors[3]. For these reasons, we anticipate the synthesis of a variety of other novel carbon forms from such lyotropic polyaromatic systems.

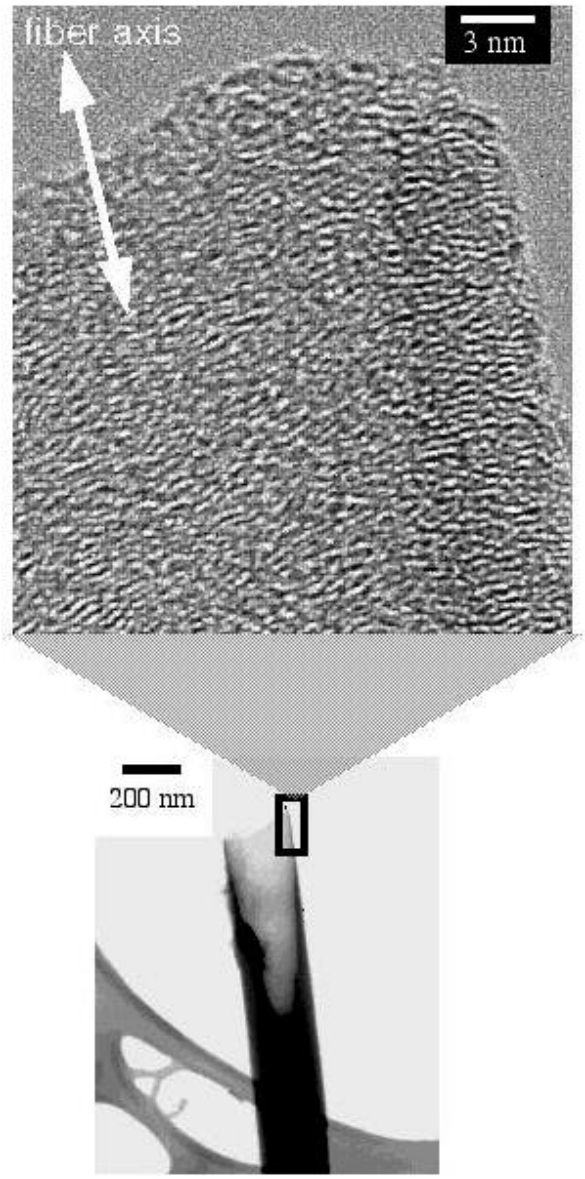

Figure 5. Perpendicular graphene layer arrangement in the thin wall sections of cellular carbon nanotubes produced from high-concentration solutions of naphthalene polymer (AR mesophase) in pyridine.

Acknowledgements

This work was supported by the National Science Foundation through a Nanoscale Interdisciplinary Research Team (NIRT) Grant at Brown University, CMS-0304246, and by the Electric Power Research Institute, Dr. A. Mehta project manager.

References

1. Harris, P.J.F., "Carbon Nanotubes and Related Structures," Cambridge University Press, Cambridge, 2001.

2. Ajayan, P.M., "Carbon Nanotubes," Chap. 8 in *Handbook of Nanostructured Materials and Nanotechnology*, H.S. Nalwa, Ed., Academic Press, New York, 2000.

3. Hurt, R.H.; Chen, Z-Y., *Physics Today*, **2000** 53 (3) 39.

4. Rodriguez, N.M.; Chambers, A.; Baker, R.T.K., *Langmuir* **1995** 11 3862.

5. Endo, M.; Kim, Y.A., Hayashi, T.; Fukai, Y., *Appl. Phys. Let.*, **2002** 80(7) 1267.

6. Gao, R.; Tan, C.D.; Baker, R.T.K.; *Catalysis Today* **2001** 65 (1) 19-29.

7. Bessel, C.A.; Laubernds, K.; Rodriguez, N.M.; Baker, R.T.K.; *J. Phys. Chem B.*, **2001** 105 (6) 1115-1118.

8. Yoon, S.H.; Park, C.W.; Yang, H.; Korai, Y.; Mochida, I.; Baker, R.T.K.; Rodriguez, N.M.; *Carbon* **2004** 42 21-32.

9. Yu, B.Z.; Li, M.K.; Lu, M.; Li, H.L.; *Appl. Phys. A* **2003** 76 593-598.

10. Martin, C.R., *Science* **1994,** 266, 1961.

11. Zhao, L.; Yang, W.; Ma, Y.; Yao, J.; Li, Y.; Liu, H.; *Chem Commun*, **2003** 2442.

12. Kyotani, T.; Tsai, L.; Tomita, A.; *Chem. Mater.* **1995** 7 1427.

13. Hulteen, J.C.; Chen, H.X.; Chambliss, C.K.; Martin, C.R., *NanoStructured Materials,*
1997 9 133.

14. Jian, K., Shim, H.-S., Schwartzman, A., Crawford, G.P., Hurt, R.H., *Adv. Mater.* **15** (2) 164-167 (2003).

15. Iverson, I.K.; Casey, S.M.; Seo, W.; Tam-Chang S., *Langmuir* **2002** 18 3510.

16. A. Dembo, A. Ionov, P.Lazarev, A. Manko, V. Nazarov, *Mol. Mater.* **2001** 14 275-290.

17. Lazarev P., Lokshin, K., Nazarov, V., *Mol Mater.* **2001** 14 303-311.

18. Boenigk W.; Haenel, M.W.; Zander, M.; *Carbon*, **1995** 74 (2) 305-306.

19. Jian, K.; Shim, H.S.; Tuhus-Dubrov, D.; Woodward, C.; Bernstein, S.; Pfeffer, M.; Steingart, D.; Sachsmann, S.; Gournay, T.; Crawford, G.P.; Hurt, R.H.; *Carbon*, **2003** 41 (11) 2073.

20. Hurt, R.H.; Krammer, G.; Crawford, G.; Jian, K.; Rulison, C.; *Chem. Mater*, **2002** 14 4558.

21. Deinhammer R.S., Ho Mankit, Anderegg J.W., Porter, M.D., *Langmuir* **10** 1306-1313 (1994).